

*J. Electroanal. Chem.*, 328 (1992) 47–62  
Elsevier Sequoia S.A., Lausanne  
JEC 01996

## Scanning electrochemical microscopy

### Part 13. Evaluation of the tip shapes of nanometer size microelectrodes

Michael V. Mirkin, Fu-Ren F. Fan and Allen J. Bard

*Department of Chemistry and Biochemistry, The University of Texas at Austin, Austin, TX 78712 (USA)*

(Received 7 October 1991; in revised form 12 December 1991)

#### Abstract

The shape of steady-state current–distance ( $i_T-d$ ) curves obtained by scanning electrochemical microscopy (SECM) with a submicrometer conical-type tip is substantially different from that obtained with a microdisk tip. A model is proposed to describe the  $i_T-d$  curves for tips shaped as cones or spherical segments. In each case a family of theoretical working curves, computed for different values of a single adjustable parameter (the height of a cone or a segment), was used to fit the experimental curves obtained with tips approaching a conductive or insulating substrate. A good fit of the experimental and theoretical curves can be obtained only for a very narrow range of the tip shape parameters, giving confidence in the reliability of the proposed method. The shape parameters for two substantially different microelectrodes are evaluated. A 420 nm radius tip was shown to be a fairly sharp cone with a height-to-radius ratio  $k$  of 0.8. An 80 nm radius tip can be represented as either a cone or spherical segment, because of the small  $k = 0.2$ . The radius values obtained from  $i_T-d$  curves agree with those estimated from steady-state current values. The cyclic voltammograms (CVs) obtained at these microtip electrodes have a regular shape with very small capacitive and resistive background. New analytical approximations for  $i_T-d$  curves are also proposed for SECM with a disk-shaped tip over conductive and insulating substrates.

#### INTRODUCTION

This paper deals with an approach to determining the shape of an ultramicroelectrode from its scanning electrochemical microscopy (SECM) response. Ultramicroelectrodes possess many advantages for studying electrochemical kinetics [1,2], and in electroanalytical applications [1,2], imaging [3] and surface modification [4]. The rate of mass transport at very small electrodes is so high that kinetic measurements can be carried out by steady-state measurements rather than

transient techniques [5]. By decreasing the size of a microelectrode from the micrometer to the nanometer range, the study of the kinetics of very fast electrochemical and chemical reactions should be possible. The electrode size is also critical for electrochemical imaging and is the main parameter determining the resolution in SECM [6–8]. Different methods of making very small electrodes have been proposed. White and coworkers [9] manufactured microband electrodes as small as 20–500 Å wide; these are promising for kinetic measurements, but cannot be used as SECM tips. Very small disk-shaped electrodes have a number of advantages—their surface is quite reproducible and well-established theory for mass transport and kinetics is available for this type of geometry [1,10]. The latter is especially important for SECM, because the theory of SECM response is developed only for a disk-shaped tip [11–13]. While nominally disk-shaped electrodes can be made with radii in the micrometer range, it is difficult to construct and characterize very small (nanometer range) insulated electrodes with a disk shape [1]. It is also difficult to sharpen conically the glass wall surrounding such a small disk so that it can be used as an SECM tip and can be moved close to a substrate without the insulating portion striking the substrate surface [7,14]. The preparation of spherically or conically shaped ultramicroelectrodes is easier. For example, Penner et al. [15] reported the fabrication of very small electrodes (“nanodes”). These were made by electrochemically etching a Pt + Ir wire to produce a tapered tip and then pushing this through molten glass to insulate most of the wire. For these small electrodes one cannot obtain good images by electron microscopy techniques. These authors estimated values of standard electrochemical rate constants with these electrodes from steady-state voltammograms, assuming a hemispherical shape of the electrodes. However, the actual shapes of these may be closer to cones (or disks) than to hemispheres. Although the shape of a reversible steady-state voltammogram is the same for a hemisphere and the equivalent size disk, this is not true for quasi-reversible or irreversible voltammograms [16]. The theory for CVs at a spherical segment (less than a hemisphere) or conical electrode has not been reported, and one cannot estimate the error in the radius and  $k_s$  values due to the geometrical uncertainties. Thus voltammetric measurements with very small electrodes are not straightforward [17] because it is difficult to evaluate their shape by the usual electrochemical measurements or any kind of microscopy.

The same problems arise in SECM experiments with submicron conical tips [18], where it is necessary to characterize the shape of the microelectrode in order to treat the SECM response. An approximate treatment based on a thin-layer cell theory [19] showed that, unlike the single working electrode experiments, the shape of SECM current–distance curves should depend dramatically upon the tip geometry. The diffusion to a small electrode (hemisphere, cone, disk) rapidly attains hemispherical diffusion when the electrode is far from any substrate. However, when it is positioned close (i.e. within a few radii) to a flat substrate, the different distances between different parts of the electrode (tip) and substrate lead to responses that are a function of tip shape. Thus the SECM can be used to

evaluate ultramicroelectrode geometry, even for tips that cannot be imaged with a scanning electron microscope. While traditionally the SECM is used to characterize an unknown substrate surface using a well-defined tip electrode, we now solve the inverse problem: characterization of the tip shape using an SECM feedback signal from a well-defined flat substrate.

## THEORY

The rigorous description of SECM with a tip shaped either as a cone or spherical segment would require solving a rather complicated diffusion problem. Even for the much simpler situation of a single spherical segment electrode without a substrate in the proximity of the tip, no theory is available and only an empirical expression for diffusion-controlled steady-state current has been proposed [20]. Aoki [21] has solved the time-dependent problem for a diffusion-controlled process at a conical electrode. He obtained a quite complicated exact expression for current in the Laplace transform domain, which was not used to compute any data for  $i-t$  curves, and also a long-time approximation for a sharply spired electrode, which is not relevant to the present study. Moreover, solving the conical/spherical SECM problem exactly would be worthwhile only if the actual tip was precisely a cone or a spherical segment. Since this is not the case, we have developed only an approximate treatment of the problem.

### *Analytical approximations for SECM with a disk-shaped tip*

The theory for a conical or spherical SECM tip is developed below using the dependencies of the diffusion-controlled steady-state current  $i_T$  on the tip-substrate distance  $d$  (over conductive or insulating substrates) tabulated in ref. 11. Since we integrate these functions, their analytical approximations are desirable. The analytical expression for a conductive substrate, given in ref. 11 with an accuracy to 2%, can be improved and an analytical approximation for an insulating substrate is also possible. We find that

$$i_T(L)/i_{T,\infty} = 0.68 + 0.78377/L + 0.3315 \exp(-1.0672/L) \quad (1)$$

where  $L = d/a$  is the normalized distance between the conductive substrate and the tip of radius  $a$ , fits within 0.7% the  $i_T-d$  curve [11] over an  $L$  interval from 0.05 to 20. For an insulating substrate a similar equation

$$i_T(L)/i_{T,\infty} = 1/[0.292 + 1.5151/L + 0.6553 \exp(-2.4035/L)] \quad (2)$$

is slightly less accurate (within 1.2%); however the longer expression

$$i_T(L)/i_{T,\infty} = 1/\{(0.15 + 1.5385/L + 0.58 \exp(-1.14/L) + 0.0908 \exp[(L - 6.3)/(1.017L)]\} \quad (3)$$

is accurate to within 0.5% over the same  $L$  interval.

### Spherical segment tip

Equations (1)–(3) were derived using the data tabulated in ref. 11 for RG (the ratio of the insulating sheath radius to that of the tip electrode) equal to 10, as was assumed in most of the previous theoretical and experimental work on SECM [3,8,12]. This value is probably somewhat larger than actual tip RG values (typically about 2–5 to allow the attainment of small tip–substrate separations without the insulator contacting the substrate). The size of RG is unimportant for a conductive substrate, and for  $RG < 10$  the normalized steady-state current is only weakly dependent on RG for insulators [10]. The response of conically or spherically shaped tips, discussed below, should be even less sensitive to RG because the insulating sheath in this case does not approach the substrate surface closely. In ref. 19 approximate expressions were obtained for the steady-state current in a thin-layer cell formed by two electrodes, for example, one a plane and the second a cone or hemisphere. The surface of the nonplanar electrode was considered to be a series of thin circular strips, each of which is parallel to the planar electrode. The diffusion current to each strip was given by the equation for thin-layer parallel-plate electrodes:

$$\Delta i = \text{const}/d \quad (4)$$

where  $d$  is the distance between the given strip and the planar electrode. This model contains an assumption that the diffusion flux of electroactive species between the tip and the substrate is essentially normal to the substrate plane. The validity of this assumption follows from the exact treatment [8].

It was shown later [11] that the thin-layer theory does not describe accurately the steady-state current between a small disk tip and a planar substrate. Therefore in this work we use SECM expressions [11] for the  $\Delta i(d)$  function rather than eqn. (4). In the case of a spherical segment tip (Fig. 1) the surface area of the strip is

$$\Delta A = 2\pi r \Delta r \quad (5)$$

where  $r$  is the radius of a circular strip, or, using the angle  $\alpha$  as an independent variable,

$$\Delta A = 2R \sin \alpha \cos \alpha \Delta \alpha \quad (6)$$

where  $R$  is the sphere radius. The distance between the strip and the substrate is

$$d = d_0 + R(1 - \cos \alpha) \quad (7)$$

where  $d_0$  is the distance between the substrate and the point of the tip closest to it. The normalized current to the whole surface of the segment can be expressed as

$$I(L) = i_T(L)/i_{T,\infty} = \frac{2}{\sin^2(\alpha_0)} \int_0^{\alpha_0} i_{\text{disk}}(z) \sin \alpha \cos \alpha \, d\alpha \quad (8)$$

where  $i_T(L)$  is the tip current at the normalized distance  $L = d_0/r_0$  from the substrate,  $i_{T,\infty}$  is the tip steady-state current at an infinite distance from the

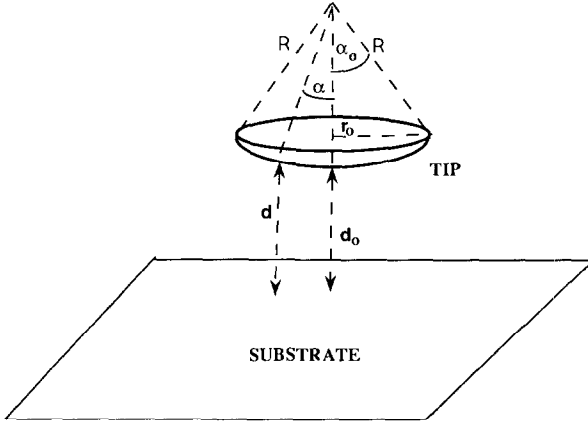


Fig. 1. Scheme of a thin-layer cell formed by a spherical segment tip and a planar substrate.

substrate,  $\alpha_0$  is the maximum value of  $\alpha$ ,  $r_0 = R \sin \alpha_0$  is the segment base radius,  $z = d/r_0 = d_0/r_0 + (1 - \cos \alpha)/\sin \alpha_0$  and  $i_{\text{disk}}(z)$  is the SECM current function  $i_T/i_{T,\infty}$  [11] which can be computed from eqn. (1) or eqn. (3) for conductive and insulating substrates respectively. With the new variable  $y = \cos \alpha$ , eqn. (8) becomes simpler:

$$I(L) = \frac{2}{\sin^2(\alpha_0)} \int_{\cos \alpha_0}^1 i_{\text{disk}}(z) y \, dy \quad (9)$$

Two families of working curves, for conductive (Fig. 2) and insulating (Fig. 3) substrates, were obtained from eqn. (9) for 20 values of the parameter  $\alpha_0$  from  $\pi/40$  to  $\pi/2$  and for the interval of normalized distance  $L$  from 0.01 to 16. One can see that the different working curves possess substantially different curvature; thus a unique curve can be found to obtain the best fit with the experimental data. The upper curve in Fig. 2 and the lower one in Fig. 3 represent the theory for a microdisk tip [11]. Obviously, as  $\alpha_0 \rightarrow 0$  the spherical segment working curves approach that computed for a disk-shaped tip.

### Conical tip

In the case of conical geometry, an analogous approach (Fig. 4) leads to the following expressions for the strip surface area and the distance between the strip and the substrate:

$$\Delta A = \frac{2\pi r_0^2 h \Delta h}{h_0^2} \quad (10)$$

$$d = d_0 + h \quad (11)$$

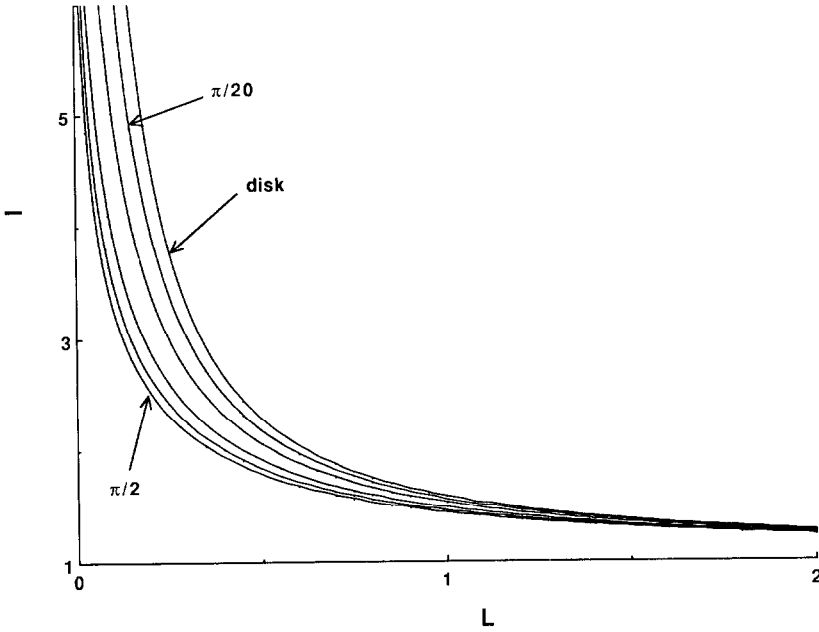


Fig. 2. Steady-state current–distance curves for a spherical segment tip over a planar conductive substrate corresponding to different values of the angle  $\alpha_0$ , and the analogous working curve for a disk-shaped tip. From bottom to top,  $\alpha_0$  is  $\pi/2$ ,  $7\pi/20$ ,  $\pi/4$ ,  $\pi/8$  and  $\pi/20$ . The upper curve is computed for a disk-shaped tip from eqn. (1).

where  $h$  is the distance from the top of the cone to the strip,  $h_0$  is the height of the cone and  $r_0$  is the radius of its base. The final expression for normalized current is

$$I(L) = \frac{2}{k^2} \int_0^k i_{\text{disk}}(z) y \, dy \quad (12)$$

where  $y = h/r_0$ ,  $k = h_0/r_0$ ,  $L = d_0/r_0$  and  $i_{\text{disk}}(z)$  is taken from eqn. (1) or eqn. (3) at  $z = L + y$ .

Two families of working curves, for conductive (Fig. 5) and insulating (Fig. 6) substrates, were computed from eqn. (12) for 20 values of the parameter  $k$  from 0.1 to 5 and for the interval of  $L$  from 0.01 to 16. The difference between the conical working curves and the disk curve (the upper curve in Fig. 5 and the lower one in Fig. 6) is larger than in the case of a spherical segment. This difference is due to the effect of the sharp tip of the cone. The triangle points in Fig. 5 were computed using eqn. (9) of ref. 19, which is based on a thin-layer approximation, for the same  $k$  value as that in curve 4. As expected, at very small tip–substrate separation, both treatments lead to similar values of the normalized current. At large  $L$  the difference increases and tends to unity as  $L \rightarrow \infty$ . This limiting value corresponds to the tip steady-state current  $i_{T,\infty}$ , which was not included in the

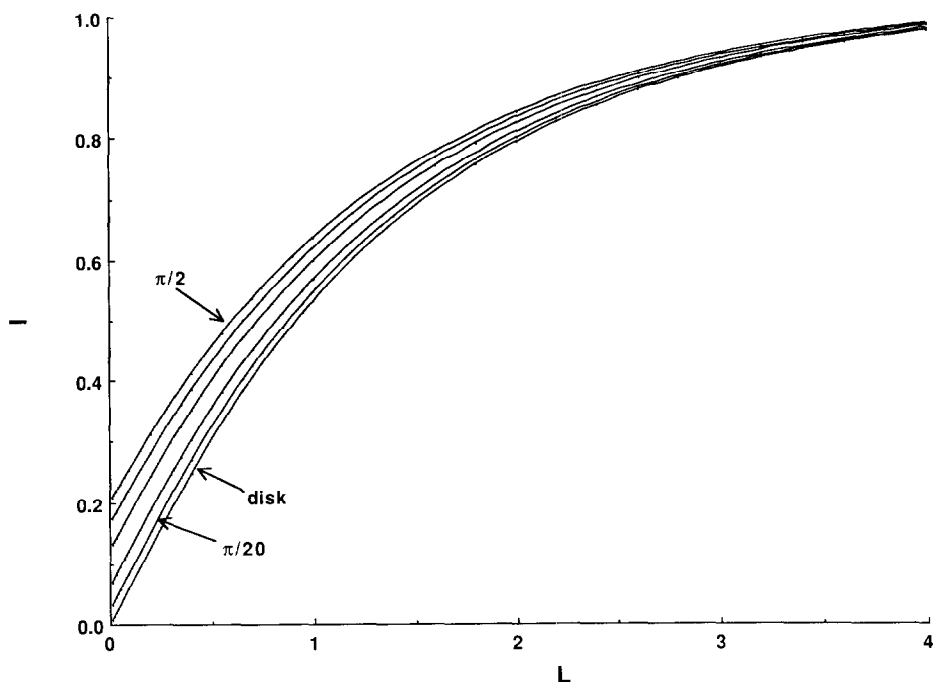


Fig. 3. The same family of curves as in Fig. 2 but for an insulating substrate. From top to bottom,  $\alpha_0$  is  $\pi/2$ ,  $7\pi/20$ ,  $\pi/4$ ,  $\pi/8$  and  $\pi/20$ . The lower curve is computed for a disk-shaped tip from eqn. (3).

earlier model [19]. It should be noted, however, that at small distances both models predict a levelling off of the normalized current at a cone compared with a disk. This range of  $L$  may be difficult to examine with actual very small tips because of the onset of tunneling between tip and substrate when  $d \approx 10\text{--}20 \text{ \AA}$ .

## EXPERIMENTAL

### Material

Tris(2,2'-bipyridyl) osmium(II) ( $\text{Os}(\text{bpy})_3^{2+}$ ) was synthesized according to previously reported procedures [22].  $n\text{-WSe}_2$  single crystals were synthesized by chemical vapor transport [23]. The substrate, a Pt disk (diameter, 5 mm) with a Pt wire spot-welded to one side, was polished successively with 5, 1 and  $0.25 \mu\text{m}$  diamond compounds and finally with  $0.05 \mu\text{m}$  alumina. After boiling in concentrated  $\text{HNO}_3$  for 15 min, it was washed with Millipore reagent water and then annealed in a  $\text{H}_2 + \text{O}_2$  flame for about 1 h and subsequently quenched in deoxygenated Millipore reagent water. All other chemicals were reagent grade and were used without further purification. Millipore reagent water was used for the preparation of

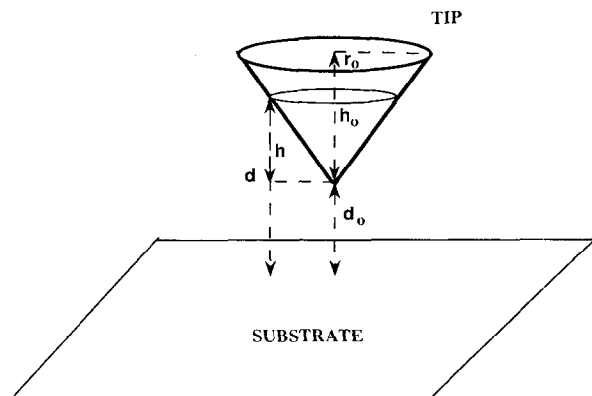


Fig. 4. Scheme of a thin-layer cell formed by a conical tip and a planar substrate.

aqueous solutions. If not otherwise mentioned, all solutions were deoxygenated for at least 30 min with purified nitrogen before each experiment. These experiments were carried out with the solution under a nitrogen atmosphere. Pt + Ir rods (0.125 mm in diameter) were obtained from the FHC Co. (Brunswick, ME).

#### *Microtip preparation*

A 125  $\mu\text{m}$  diameter Pt + Ir rod was sharpened by electrochemical etching in a solution consisting of saturated  $\text{CaCl}_2$  (60 vol.%),  $\text{H}_2\text{O}$  (36 vol.%) and HCl (4 vol.%) at approx. 25 V root mean square (rms) ac applied with a Variac transformer [24]. A carbon rod served as the counter-electrode in a two-electrode cell. After etching, the microtips were washed with Millipore reagent water and ethanol, and then dried in air prior to insulation. The tips were insulated with molten Apiezon wax following the procedures reported by Nagahara et al. [25]. Several coatings were usually required to insulate the tip completely or nearly completely. The degree of insulation of a tip was checked by carrying out cyclic voltammetry in a solution containing a redox species. For a well-insulated tip, no detectable voltammetric waves were obtained. The very end of a completely insulated tip could be exposed by placing it in a scanning tunneling microscope (STM) with a bias voltage (e.g. 10 V) applied between the tip and a conductive substrate (e.g. a Pt disk). The onset of current flow (e.g. 0.5 nA) produced a hole in the tip insulation at the point of closest approach of tip to substrate, while leaving most of the tip still insulated. The exposed area of the tip could be controlled by the bias voltage and the onset current flow. We could usually successfully obtain STM images on conductive surfaces with these tips. A further treatment of "micropolishing" these tips by continuously scanning them over the substrate could enlarge the exposed area relative to those without this treatment. The use of these tips for imaging will be described elsewhere.

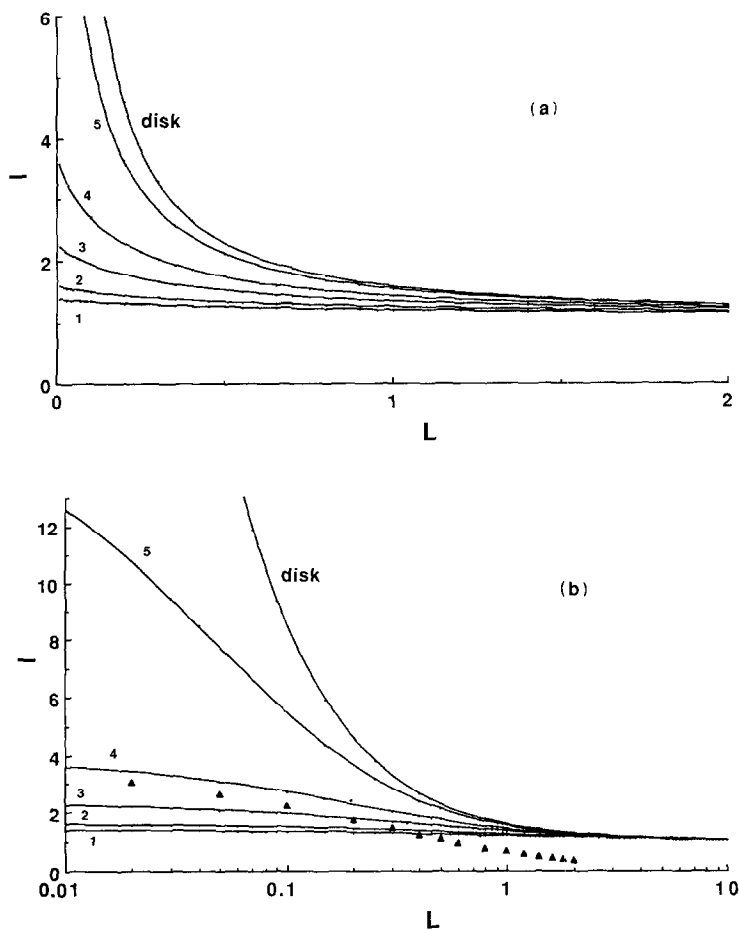


Fig. 5. (a) Steady-state current–distance curves for a conical tip over a planar conductive substrate corresponding to different values of the parameter  $k = h_0/r_0$  and the analogous working curve for a disk-shaped tip:  $k$  values of 3 (1), 2 (2), 1 (3), 0.5 (4) and 0.1 (5). The upper curve is computed for a disk-shaped tip from eqn. (1). (b) The same data on a semilogarithmic scale: ▲ computed from eqn. (9) in ref. 19 with the same parameter values as in curve 4.

### Apparatus

STM, SECM and electrochemical measurements were performed using an instrument described previously [26]. Voltage sweeps were performed using a PAR 175 universal programmer and an IBM EC225 voltammetric analyzer. Data were collected and processed via a personal computer.

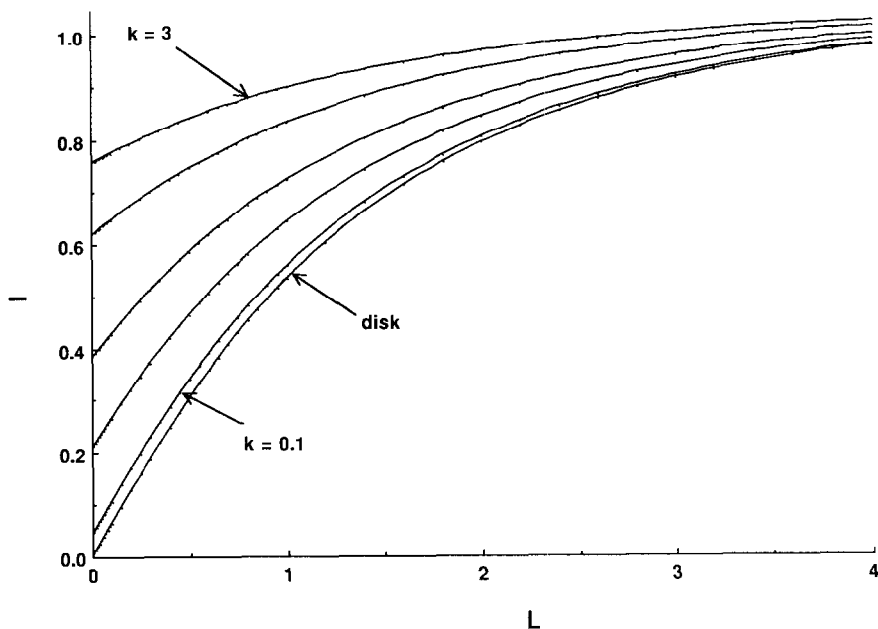


Fig. 6. The same family of curves as in Fig. 5, but for an insulating substrate. From top to bottom  $k$  is 3, 2, 1, 0.5 and 0.1. The lower curve is computed for a disk-shaped tip from eqn. (3).

## RESULTS AND DISCUSSION

The lateral resolution of the SECM is governed by the size and shape of the microtip electrode and the ability to bring it into close proximity to the substrate surface [6]. To increase the lateral resolution of the SECM, it is crucial that SECM microtip electrodes have an appropriate geometry and a small exposed area. The active tip area must be at the lowest point of the electrode structure. It is thus beneficial to minimize the diameter of the insulation (denoted RG in ref. 11) and to allow the active tip area to protrude slightly beyond the plane of the insulation. The microtips described here apparently fulfill these requirements and can be used for both STM and SECM imaging. However, the determination of the size and geometry of these microtips becomes difficult, even by scanning electron microscopy, because of the small dimension and the coated Apiezon wax layer. In an earlier paper [19], we showed that the normalized steady-state diffusion-limited current, as a function of the normalized separation for thin-layer electrochemical cells, is fairly sensitive to the geometry of the electrodes. This geometry dependence, combined with cyclic voltammetry, can be used to quantitate the degree of exposed tip and describes some aspects of the coatings.

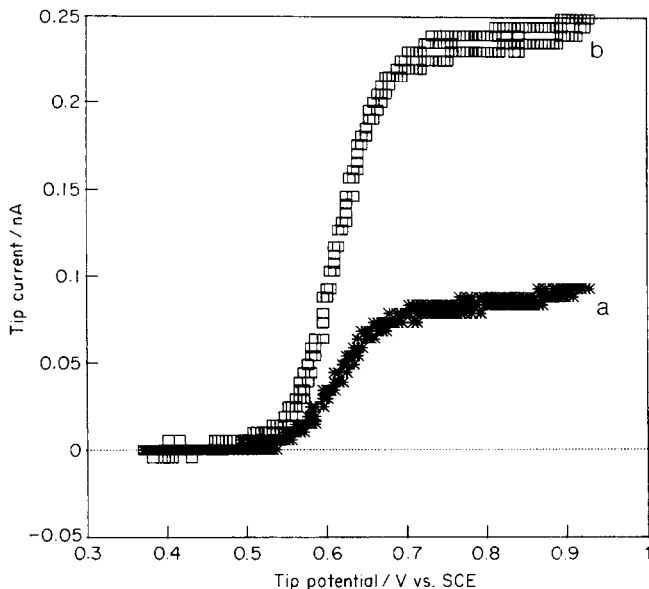


Fig. 7. CVs at a microtip electrode at (a) an infinite distance and (b) 35 nm away from a Pt substrate (diameter, 5 mm) in a solution containing 1.5 mM  $\text{Os}(\text{bpy})_3^{2+}$  and 0.5 M  $\text{Na}_2\text{SO}_4$  as the supporting electrolyte. Scan rate,  $100 \text{ mV s}^{-1}$ . The substrate was held at 0.2 V/SCE.

### Cyclic voltammetry

The electrodes were first characterized by cyclic voltammetry. Figure 7 shows CVs for a microtip electrode in a solution containing 1.5 mM  $\text{Os}(\text{bpy})_3^{2+}$  and 0.5 M  $\text{Na}_2\text{SO}_4$  supporting electrolyte. The radius  $a$  of a disk with an area equal to the effective exposed area of the microtip electrode can be estimated by the diffusion-limited steady-state current  $i_{\text{disk}}^{\infty}$  by using the relation [1]

$$i_{\text{disk}}^{\infty} = 4nFaDc \quad (13)$$

where  $n$  is the number of electrons transferred per molecule,  $F$  is the Faraday constant and  $D$  and  $c$  are the diffusion coefficient and the bulk concentration of the redox species respectively. The effective disk radius of this electrode is calculated to be about 420 nm by taking  $D$  of  $\text{Os}(\text{bpy})_3^{2+}$  as  $3.9 \times 10^{-6} \text{ cm}^2 \text{ s}^{-1}$  [27]. It should be noted that the exact value of the radius cannot be obtained from eqn. (13) because (i) the actual tip does not possess a disk geometry, (ii) the geometry of the insulator surrounding the tip is unknown and (iii) the very small surface of the tip cannot be polished and may therefore be partially blocked by impurities. For the Pt + Ir microtip electrodes prepared here, the effective radius spanned a range from a few nanometers to  $1 \mu\text{m}$ . The CVs obtained at an infinite tip–substrate separation (Fig. 7) have shapes typical of a hemispherical or disk-

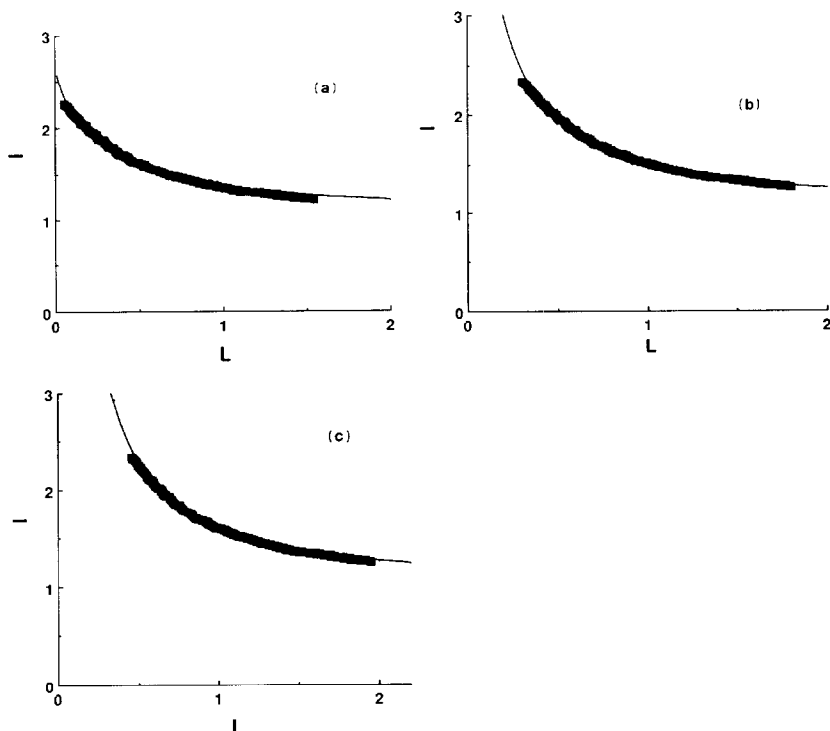


Fig. 8. Normalized tip current vs. normalized distance for a tip electrode over a conductive substrate (a Pt disk) in a solution containing 1.5 mM  $\text{Os}(\text{bpy})_3^{3+}$  and 0.5 M  $\text{Na}_2\text{SO}_4$  as the supporting electrolyte (thick curve). The Pt substrate (diameter, 5 mm) was held at 0.2 V SCE;  $i_{T,\infty} = 0.059$  nA. The thin curves show the theoretical curves computed for (a) conical 420 nm radius tip,  $k = 0.8$  and offset = 0, (b) spherical segment 420 nm base radius tip,  $\alpha_0 = 0.7069$  and offset = 105 nm and (c) 420 nm radius disk tip and offset = 170 nm.

shaped microelectrode with a very small capacitive and resistive background. One can also see from Fig. 7 that the steady-state tip current depends strongly on  $d_0$ , so that these tips are suitable for SECM imaging.

#### *Tip current–distance relation*

The normalized tip current, as a function of the normalized tip–substrate distance, for a conductive substrate (e.g. Pt in the present case), is shown in Fig. 8. The experiment was carried out with an aqueous solution containing 1.5 mM  $\text{Os}(\text{bpy})_3^{2+}$  and 0.5 M  $\text{Na}_2\text{SO}_4$  as the supporting electrolyte. During the distance scan, the tip was held at 0.80 V vs. a saturated calomel electrode (SCE), where a steady-state plateau was obtained in the CV, and the Pt substrate was biased at 0.20 V SCE, where  $\text{Os}(\text{bpy})_3^{3+}$  generated at the tip was reduced back to  $\text{Os}(\text{bpy})_3^{2+}$ .

The steady-state current value  $i_{T,\infty} = 0.059 \pm 0.001$  nA obtained at an infinite tip–substrate separation suggests the radius value to be in the range of 200–500 nm. We tried three ways of fitting these experimental data using the families of theoretical current–distance curves computed for conical (eqn. (12)) and spherical (eqn. (9)) geometries, as well as a disk curve (eqn. (1)). Three parameters can be varied for conical or spherical geometry, i.e. the radius, the height parameter ( $k$  or  $\alpha_0$ ) and the “offset” value. In the case of a disk only two parameters,  $r_0$  and the offset, are applicable. The offset characterizes an error in zero-distance determination. In a conventional SECM experiment with a disk tip embedded in an insulating sheath, the point of zero tip–substrate separation cannot be determined exactly because small protrusions in the insulating sheath, or lack of precise alignment of the tip with respect to the substrate, will often cause the insulator to touch the substrate before the actual  $d = 0$  is reached. The distance scale is thus usually obtained by an arbitrary adjustment of the  $i_T$ – $d$  curve to fit the theoretical response for a disk. However, with the tips described here the actual zero-point can be evaluated within a few nanometers, and any errors in the  $d = 0$  value should be in this range if the shape of the tip is correctly determined.

The fitting procedure showed that the radius value is in fact not an adjustable parameter; a good fit can be obtained only for some fixed-radius value. This value appeared to be constant whether the simulation is based on a conical, spherical or disk approximation. The experimental current–distance curve shown in Fig. 8 can be fitted using conical (Fig. 8(a)), spherical segment (Fig. 8(b)) or disk (Fig. 8(c)) approximations with the same radius value  $r_0 = 420$  nm and  $k = 0.8$  or  $\alpha_0 = 0.7069$ . The most significant difference between these three cases is the required offset value needed for a best fit which is equal to (a) 0 nm, (b) 105 nm and (c) 170 nm for cone, spherical segment and disk respectively. A geometrical interpretation of these results is given in Fig. 9(a). The equal radii of the disk, spherical segment and cone base apparently lead to the fixed-size projection on the substrate plane, and the value of this radius is essential for determination of the diffusional flux normal to this plane. The sharp top of the cone (as well as the top of a spherical segment) prevents the substrate from approaching the main part of the tip surface. The differences in the heights of these three bodies determine (qualitatively) the offset values required to fit the experimental curve using each of these approximations. We can conclude from the offset values that the actual tip looks more like a cone than a disk or a spherical segment.

The normalized tip current as a function of normalized distance was also obtained with a different tip over an n-WSe<sub>2</sub> insulating substrate under open-circuit conditions. There were two main reasons to choose an n-WSe<sub>2</sub> single crystal as a substrate. First, an atomically smooth surface could be prepared by carefully peeling off the top several layers with adhesive tape. Second, and more importantly, we could manipulate the conductance of the substrate by choice of bias voltage. It is conductive in the forward bias, and non-conductive in the reverse bias direction or on open circuit. By operating in the STM mode with n-WSe<sub>2</sub> forward biased, for example, holding the tip at 0.10 V and the n-WSe<sub>2</sub> substrate at  $-0.60$

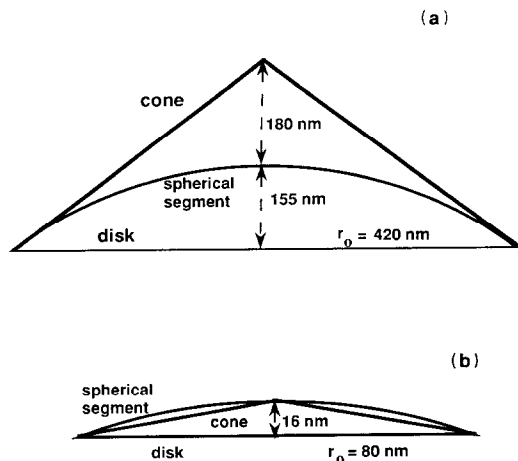


Fig. 9. Schemes of the section of the cone, spherical segment and disk used to fit the experimental curves obtained with two different tips over (a) conductive and (b) non-conductive substrates.

V SCE, the tunneling current can dominate the faradaic current and the zero distance can be determined very accurately, perhaps within 1 nm. Then if the n-WSe<sub>2</sub> electrode is left on open circuit, it will behave as an insulator. We used these conditions to obtain the tip current vs. distance curves for the insulating substrate shown in Fig. 10. The experiment was performed in a deoxygenated aqueous solution containing 0.5 M K<sub>4</sub>Fe(CN)<sub>6</sub> and 0.5 M Na<sub>2</sub>SO<sub>4</sub>. During the distance scan, the tip was held at 0.55 V SCE and the n-WSe<sub>2</sub> substrate was left on open circuit. The steady-state current value in this case,  $i_{T,\infty} = 2.24$  nA, suggests a smaller value of the tip radius in the range 20–100 nm. The fitting procedure based on the conical and spherical families of the working curves (Fig. 10(a))

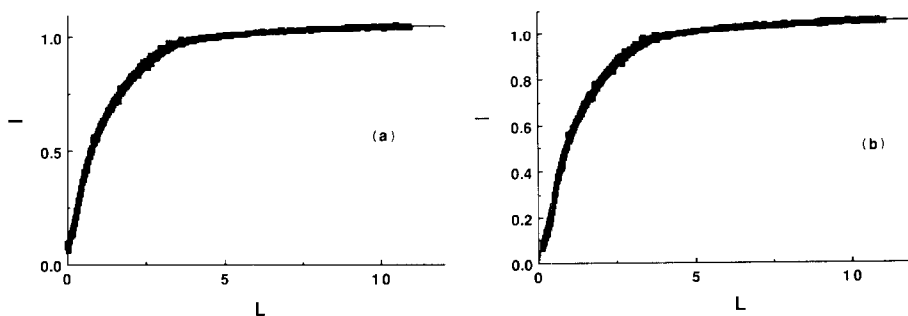


Fig. 10. Normalized tip current vs. normalized distance for a tip electrode over a nonconductive substrate n-WSe<sub>2</sub> (diameter, 2 mm) at open circuit in a solution containing 0.5 M K<sub>4</sub>Fe(CN)<sub>6</sub> and 0.5 M Na<sub>2</sub>SO<sub>4</sub>;  $i_{T,\infty} = 2.24$  nA. Thin curves show the theoretical curves computed for (a) conical 80 nm radius tip,  $k = 0.2$  and offset =  $-3$  nm and (b) 80 nm radius disk tip and offset =  $9$  nm. The curve for spherical geometry is indistinguishable from the conical curve (a).

computed from eqns. (3) and (12) or (9), and the disk (Fig. 10(b)) current–distance dependence, eqn. (3), showed the same  $r_0$  value of 80 nm for all three types of geometry. The height of this tip is small;  $k = 0.2$  for conical geometry and  $\alpha_0 = 0.3927$  for the spherical segment. These values correspond to exactly the same value of tip height;  $h_0 = 16$  nm. As a result, the same offset value of  $-3$  nm was obtained for both approximations, because there is no significant difference between a cone and a spherical segment when the height is so small (Fig. 9(b)). The offset value corresponding to the disk geometry is 9 nm, and the difference in the offset, 12 nm, is in good agreement with the  $h_0$  value found.

The approximate theory proposed here apparently provides a good description of the steady-state current–distance curves for both conductive and insulating substrates and for the whole SECM normalized distance range. It should be suitable for quantitative interpretations of high resolution SECM images obtained under conditions of diffusion control. This same approach should be applicable to electrodes with other geometries. However, exact solutions of the diffusion problems are necessary to substantiate the use of these microelectrodes for kinetic measurements. One can conclude from this example that the difference between a microdisk and a conical (or spherical) shaped tip can be detected when  $k > 0.1$ . This value is close to the typical offset for experimental current–distance curves obtained with a disk-shaped tip.

## CONCLUSIONS

We have studied the possibility of employing submicron non-disk-shaped tips for SECM experiments. While we are still not able to specify parameters which can routinely produce nanometer-sized tips, it is very likely that these tips are suitable for very high resolution SECM imaging because of their appropriate geometric shape with the small active area exposed at the lowest point of the tip. We have applied electrochemical and SECM techniques to determine the size and geometry of such tips. A good fit between the experimental and theoretical data suggests that the SECM current–distance measurement can be employed to evaluate the size and shape of microtip electrodes. We have also been able to use these tips for SECM imaging [18]. The established theory provides accurate expressions for the current–distance curves obtained with such tips, and thus can be used for quantitative interpretation of the SECM images. The results seem quite promising and experiments are currently in progress.

## ACKNOWLEDGMENTS

The support of this research by grants from the Texas Advanced Research Program, the Robert A. Welch Foundation and the National Science Foundation (CHE 8901450) is gratefully acknowledged. We are also grateful to Sam Hendricks for his assistance in the preparation of Apiezon wax coated tips.

## REFERENCES

- 1 R.M. Wightman and D.O. Wipf, in A.J. Bard (Ed.), *Electroanalytical Chemistry*, Vol. 15, M Dekker, New York, 1988, p. 267.
- 2 M. Fleischmann, S. Pons, D.R. Rolison and P.P. Schmidt, *Ultramicroelectrodes*, Datatech Sys Inc., Morgantown, NC, 1987.
- 3 A.J. Bard, G. Denuault, C. Lee, D. Mandler and D.O. Wipf, *Acc. Chem. Res.*, 23 (1990) 257, references cited therein.
- 4 D. Mandler and A.J. Bard, *Langmuir*, 6 (1990) 1489, and references cited therein.
- 5 A.M. Bond, K.B. Oldham and C.G. Zoski, *J. Electroanal. Chem.*, 216 (1989) 177.
- 6 J. Kwak and A.J. Bard, *Anal. Chem.*, 61 (1989) 1794.
- 7 C. Lee, C.J. Miller and A.J. Bard, *Anal. Chem.*, 63 (1991) 78.
- 8 A.J. Bard, M.V. Mirkin, P.R. Unwin and D.O. Wipf, *J. Phys. Chem.*, 96 (1992) 1861.
- 9 R.B. Morris, D.J. Franta and H.S. White, *J. Phys. Chem.*, 91 (1987) 3559.
- 10 M.V. Mirkin and A.J. Bard, *J. Electroanal. Chem.*, 323 (1992) 1.
- 11 J. Kwak and A.J. Bard, *Anal. Chem.*, 61 (1989) 1221.
- 12 P.R. Unwin and A.J. Bard, *J. Phys. Chem.*, 95 (1991) 7814.
- 13 M.V. Mirkin and A.J. Bard, *J. Electroanal. Chem.*, 323 (1992) 29.
- 14 A.J. Bard, F.-R.F. Fan, J. Kwak and O. Lev, *Anal. Chem.*, 61 (1989) 132.
- 15 R.M. Penner, M.J. Heben, T.L. Longin and N.S. Lewis, *Science*, 250 (1990) 1118.
- 16 K.B. Oldham and C.G. Zoski, *J. Electroanal. Chem.*, 256 (1988) 11.
- 17 A.S. Baranski, *J. Electroanal. Chem.*, 307 (1991) 287.
- 18 F.-R.F. Fan and A.J. Bard, unpublished results, 1991.
- 19 J.M. Davis, F.-R.F. Fan and A.J. Bard, *J. Electroanal. Chem.*, 238 (1987) 9.
- 20 Z. Stojek and J. Osteryoung, *Anal. Chem.*, 61 (1989) 1305.
- 21 K. Aoki, *J. Electroanal. Chem.*, 281 (1990) 29.
- 22 J.G. Gaudiello, P.R. Sharp and A.J. Bard, *J. Am. Chem. Soc.*, 104 (1982) 6373.
- 23 F.-R. Fan and A.J. Bard, *J. Electrochem. Soc.*, 128 (1981) 945.
- 24 A.A. Gewirth, D.H. Craston and A.J. Bard, *J. Electroanal. Chem.*, 261 (1989) 477.
- 25 L.A. Nagahara, T. Thundat and S.M. Lindsay, *Rev. Sci. Instrum.*, 60 (1989) 3128.
- 26 F.-R. Fan and A.J. Bard, *J. Electrochem. Soc.*, 136 (1989) 3216.
- 27 M. Rodriguez and A.J. Bard, *Anal. Chem.*, 62 (1990) 2658.